Purkinje Cell Morphology and Display Complexity in Manakins (Pipridae)

By:
Mary Claire Harvey

A thesis submitted to the faculty of The University of Mississippi in partial fulfillment of the requirements of the Sally McDonnell Barksdale Honors College.

Oxford
May 2018

Approved by:

_____
Advisor: Dr. Lainy Day

_____
Reader: Dr. Jason Hoeksema

_____
Reader: Dr. Christopher Leary

ACKNOWLEDGEMENTS

While there is no way I could possible thank everyone that has in some way impacted me or helped me on the journey of researching and producing my thesis, I would like to begin by thanking my parents and friends for their unwavering support throughout this endeavor. I am eternally grateful. I would also like to thank Michael Scott for teaching me that the only limits we face are the ones we define for ourselves. I would like to thank the fellow Day lab members for both their research contributions and support. I am especially grateful for the Sally McDonnell Barksdale Honors College for both their financial support and encouragement during my tenure at the University of Mississippi. I greatly appreciate the opportunities the SMBHC has afforded me to present my research at the Mississippi Academy of Sciences meeting and J.B. Johnston Club for Evolutionary Neurobiology meeting, as well as the opportunity to attend the annual Society for Neuroscience meeting. I would like to thank my readers, Dr. Jason Hoeksema and Dr. Christopher Leary for their contributions to my thesis. Finally, I would like to thank Dr. Lainy Day for providing me the opportunity to research in her lab for the last two years, and for her time and help in producing my thesis.

ABSTRACT
MARY CLAIRE HARVEY: Purkinje Cell Layer Morphology and Display Complexity in Manakins
(Under the direction of Dr. Lainy Day)

Manakins are a suboscine, lekking bird of the tropical and subtropical regions of South and Central America that perform complex mating displays shaped by sexual selection. The complexity of the mating display varies greatly across species of manakins. Some manakins only perform a limited number of different motor elements, whereas others have elaborate displays that consist of acrobatic movements and mechanical sound production. The complexity of these displays has been found to be positively related to brain weight, brain volume, arcopallium volume, body weight, and tarsus size but shows no relationship to the nucleus rotundus or nucleus taeniae. The volume of the cerebellum is also positively related to display complexity. The cerebellum is a neural structure that functions in coordinating motor control and motor learning. The cerebellum is made up of the cerebellar cortex and the deep cerebellar nuclei. The cerebellar cortex is divided into major layers: the molecular layer, granular cell layer, and Purkinje cell layer. Cells within these layers are homogeneously distributed across the cerebellum and perform distinct functions in cerebellar signal processing. We hypothesized that the output cells of the cerebellum, the Purkinje cells, may play a prominent role in driving the positive relationship between overall cerebellar volume and display complexity. We quantified Purkinje cell number and cell volume in 6 manakin species, and Purkinje cell layer volume in 12 species of manakins and used the

closely related ochre-bellied flycatcher as an outgroup. We found a positive relationship between Purkinje cell number and display complexity within manakins upon exclusion of the flycatcher outgroup. Neither Purkinje cell layer volume nor cell volume was related to display complexity. Purkinje layer data was analyzed alone and in the context of a larger data set showing other brain region and body size measurements that are positively associated with display complexity in these individuals. Results are discussed in this context as well as in relationship to Purkinje cell and cerebellar function.

TABLE OF CONTENTS

LIST OF TABLES AND FIGURES

LIST OF ABBREVIATIONS

CB	Cerebellum
PC	Purkinje Cell
PCLvol	Purkinje Cell Layer Volume
PCvol	Purkinje Cell Volume
PCnum	Purkinje Cell Number
ROI	Region of Interest
ASF	Area Sampling Fraction
TSH	Thickness Sampling Fraction
CE	Coefficient of Error
CBvol-PCLvol	Cerebellum volume minus Purkinje Cell Layer volume
WBvol-PCLvol	Whole Brain volume minus Purkinje Cell Layer volume
NTn	Nucleus Taeniae
GLM	General Linear Model
NTn-PCLvol	Nucleus Taeniae volume minus Purkinje Cell Layer volume

Background

Across the animal kingdom, different behaviors have shown to be a catalyst for evolutionary adaptations in neural morphology. This relationship between behavior and neural morphology is seen in Manakins (Pipridae), small suboscine passerine birds that reside in the American tropics. Many species of manakins depend on the execution of an elaborate courtship display for mating success. The manakin mating display is a lekking display where males gather in a display space to compete for attention of onlooking females (Duval, 2007, Prum, 1994). The dependence on the complexity and speed of this display for male mating success has been observed in select manakin species (Barske et al., 2011; Schlinger et al., 2013). The display can consist of hopping between branches, acrobatic flips, and production of mechanical sounds such as those made by the wings, called wing snaps (Day et al., 2014, Prum, 1994; Schlinger et al., 2013, Chapman, 1935). The degree of display complexity varies across manakin species, with some species having few display elements and others having many highly acrobatic elements. In the species we observed with the lowest number of display elements, the black manakin (*Xenopipo atronitens*), the display consists of a backflip and few additional movements, whereas in the species with the highest number of display elements, the golden-collared manakin (*Manacus vitellinus*), the display consists of multiple coordinated movements such as somersaults, hops, snap jumps, and a variety of other acrobatics (See figure 1 and table 2) (Chapman, 1935; Prum, 1998; Lindsay et al., 2015). Among manakin species, display complexity increases with the volume of the cerebellum (Pano, 2015).

In all vertebrates, the cerebellum (CB) is a neural component of the hindbrain that is critical for posture and balance as well as the learning and production of smooth coordinated motion (Thach, et al., 1992). The cerebellum is composed of the cerebellar cortex and deep cerebellar nuclei. The cerebellar cortex is divided into recognizable structures called folia and made up of three layers: the molecular layer, the Purkinje cell layer, and the granular layer. The Purkinje cell layer consists of large cells that form a single line at the convergence of the molecular and granular cell layer (Goldowitz et al., 1998, Voogd et al., 1998). The Purkinje cells serve as the sole output of the cerebellar cortex. The dendritic tree of Purkinje cells is greatly branched, extends into the molecular layer of the cerebellar cortex, and receives two types of excitatory input: mossy fibers and climbing fibers. Mossy fibers carry information that has come from sensory receptors and synapse with granule cells that then send signals to Purkinje cells via parallel fibers. One Purkinje cell can receive signals from 80,000 parallel fibers (Konnerth et al., 1990). The other excitatory input of Purkinje cells comes from climbing fibers that have a ratio of one or two climbing fibers synapsing with each Purkinje cell (Devi et al., 2016). The Purkinje cell axons then extend through the granule-cell layer to synapse with deep cerebellar nuclei and vestibular nuclei (Butler et al.,1996, Camilli et al., 1984). Deep cerebellar nuclei then project to motor nuclei and various other brain regions (Sugihara, 2010) that influence motor control.

Evolutionary neural specializations to accomplish tasks necessary for survival have been seen widely across vertebrates. In food-storing birds that require increased spatial awareness, the hippocampus, a region that plays a role in spatial memory, has shown an increase in size when compared to birds that do not require as much spatial

awareness (Sherry, 2010, Clayton, 1998). Neural specialization has also been seen in nest building birds. Birds that build complex nests, a task that requires manipulative motor skills, show greater cerebellar foliation than birds that build simpler nests (Hall et al., 2013).

Neural adaptations have also been seen as a result of sexual selection for specific behaviors. In songbirds, sexual selection has impacted vocal song production (Marshall et. al, 2003). Zebra Finches, a songbird in which only the males produce songs, show great neural sexual dimorphism. Three neural components of the song control pathway, the hyperstriatum ventrale, the robust nucleus of the archistriatum, and the hypoglossal nucleus of medulla, have shown to have a strikingly larger volume in males than females (Nottehbohm et al., 1976). Neural adaptations have also been seen in non-songbirds. Bowerbirds are birds that construct bowers, or display sites, to attract females (Marshall, 1954). Bowerbird mating success is dependent on the complexity and composition of a bower constructed by the male bird (Borgia, 1992; Madden, 2003). A strong positive relationship between bower complexity and cerebellar size has been found, and it is believed that this positive relationship is due to the role of the cerebellum in some aspect of the display (Day et al., 2004).

Manakins, however, are of particular interest because they are subject to sexual selection based on a motorically demanding non-vocal physical display and mechanical sound production (Prum, 1998). Studying the manakins' complex non-vocal motor displays is likely to lead to better understanding of the neural morphology and neural pathways that are pertinent to the production of mechanical displays.

The manakin courtship display has been found to have various neural components. Thus far, we already know that neural and physical specializations have been seen in both male and female manakins- females show specialized visual processing centers and males show specialization in motor control circuitry (Day et al., 2011). Across the manakin species, a positive relationship between courtship display complexity and whole brain weight, arcopallium size, and cerebellar volume has been found (Lindsay et al. 2015; Helmhout, 2016; Pano, 2015), as well as body weight and tarsus size (Day et al., 2016). The arcopallium, a brain region within the avian brain associated with limbic functions of emotion, memory, and motivation (Reiner et al., 2004; Yamamoto et al., 2005) has also been found to have a positive relationship with display complexity. No relationship was found between nucleus taeniae, a nucleus in the arcopallium that is associated with limbic functions (Reiner et al., 2004) or nucleus rotundus, a visual information processing center (Acerbo et al, 2003), and display complexity (Helmhout, 2016).

Our study aims to observe and quantify the relationship between Purkinje cell morphology and display complexity. We previously found that cerebellar volume increases with display complexity in manakins (Pano, 2015); to determine if this relationship is driven by homogenous increases in cerebellar layers and cell types or by mosaic evolution, we have measured the Purkinje cell layer volume and Purkinje cell volume, and the number of Purkinje cells. We expected to find that at least one aspect of Purkinje cell morphology is positively related to display complexity, which would allow us to determine if mosaic evolution is involved in cerebellar volume increases. Our studies are among the first to find brain traits correlated with a sexually selected non-

vocal motor behavior in avians, and studying the Purkinje cell morphology will provide an interesting outlook into the pertinence of cerebellar output in manakin display production.

Materials and Methods

Sample collection and tissue preparation

Brains were collected from 12 species within the Pipridae family, and one species in the family Tyrannidae, which was included as an outgroup. This species, the ochre-bellied flycatcher (*Mionectes oleagineus*), is a suboscine bird and, like Pipridae, belongs to the suborder Tyranni within the Passerine order, performs a courtship display on a lek (Westcott, 1994) and has a similar diet of small fruits collected by foraging (Marini, 1992; Snow, et. al. 1979). For all 13 species, we measured Purkinje cell layer volume (PCLvol) for 3 individuals, except for *Corapipo gutteralis*, for which we measured 2 individuals for a total of 38 males. We measured Purkinje cell volume (PCvol) and cell number (PCnum) estimates for 9 individuals representing 6 species. See table 1 for samples sizes used for measurements.

Table 1: Sample sizes per species for measurements

Species	PC cell count & volume	PC layer volume
Chiroxiphia lanceolata		3
Chiroxiphia pareola		3
Corapipo altera	1	3
Corapipo gutturalis		2
Dixiphia pipra	1	3
Lepidothrix coronata		3
Lepidothrix suavissima		2
Manacus candei		3
Manacus vitellinus	2	3
Ceratopipra cornuto		3
Ceratopipra mentalis	1	3
Xenopipo atronitens	2	3
Mionectes oleagineus	1	3

Birds were collected in Panama and Guyana between January and August during each species' breeding season in either 2012 or 2013. Exact locations for collected sites can be found in Lindsay et al. (2015). For brain extraction, birds were overdosed with isoflurane gas, and perfused transcardially with 30 mLs of 0.1M phosphate-buffered saline followed by 40 mLs of 10% neutral-buffered formalin at 3mL/min. Brains were placed in NBF for 24 hours and then cryoprotected in 20% (w/v) sucrose in phosphate-buffered saline until they sank. Brains were then transferred to cold phosphate-buffered saline for 1-4 days and then placed in a gel block (8% w/v gelatin and 16% w/v sucrose in RO-H2O. The gel block was placed in NBF for 24 hours and cryoprotected in 30%

w/v sucrose until it sank, and brains were finally frozen on dry ice and stored in a -80 freezer in the country of origin until transferred to a -80 °C freezer at the University of Mississippi. Brains were cut at 30 microns in the sagittal plane using a cryostat, and every third slice was mounted on a slide. Slides were stained with cresyl violet to allow visualization of nissl bodies and cell nuclei.

Ethics Statement

Panama collections were made with approval from the Smithsonian Tropical Research Institute's Institutional Animal Care and Use Committee, the Autoridad Nacional del Ambiente, and the Autoridad del Canal de Panamá. Birds collected from Guyana were done so with the approval of the Guyana Environmental Protection Agency. Work done on tribal lands was done with the approval of Guyana Ministry of Amerindian Affairs. All collections and sampling procedures were approved by the Institutional Animal Care and Use Committee of the University of Mississippi.

Display Complexity

In the 13 studied species, a total of 40 different display elements were identified from previously published ethograms (Prum, 1990; Chapman, 1935; Prum, 1994; Prum 1998; DuVal, 2007, Bostwick, 2003; Duraes et. al, 2007) and our own observations aided by the use of high-speed and high definition cameras to capture footage of movement.

Table 2: Components of display complexity score

Species	Displays	Cooperation	Arena	Mechanical	Complexity
M. vitellinus	10	1	3	9	24
M. candei	9	1	3	9	23
C. mentalis	8	1	1	10	21
C. cornuta	8	1	1	6	17
C. Lanceolata	12	2	1	5	21
C. pareola	9	2	1	6	19
L. suavissima	9	2	2	5	19
L. coronata	11	2	2	0	16
C. altera	9	0	1	4	15
C. gutturalis	8	0	1	4	14
D. pipra	12	0	1	0	14
X. atronitens	3	0	1	7	12
M. oleagineus	7	0	0	0	8

Table 2: Table and table legend modified with permission (Lindsay et al., 2015,S. Karger, Basel. The complexity score is the sum of: (1) unique display elements: 40 possible discrete display traits (2) cooperation: 0 = none, 1 = simple (males display at the same time but not in concert), 2 = complex (the male display is coordinated) (3) display arena type: 1 = one or more horizontal perches or a fallen log, 2 = a loosely organized court near the ground composed of a few horizontal and vertical perches but without cleared ground, 3 = a true court with a cleared display arena, and (4) mechanical sound production: total repertoire (0–5), pulse type: 1 = single, 2 = single and multiple pulses, where sounds are produced: 1 = perched, 2 = in flight, 3 = perched and in flight.

Display complexity scores are the sum of these display elements and points for level of cooperation and types and number of mechanical sounds produced (Lindsay et al., 2015; Helmhout, 2016). Examples of postural display elements include bill-pointing, upright-body, chin-down, and horizontal posture. Dynamic display elements include the bow, rolling snap, leapfrog, and frenzied-flutter display (Prum, 1990; Lindsay et al.

2015). Up to five points were assigned based on the presence of distinct mechanical sound productions and whether these were produced during other movements. To ensure display complexity scores were unbiased, displays were scored in isolated settings by two separate scorers, with a satisfactory inter-rater rating (r=0.899; p= <0.001) (Lindsay, 2011; Helmhout, 2015).

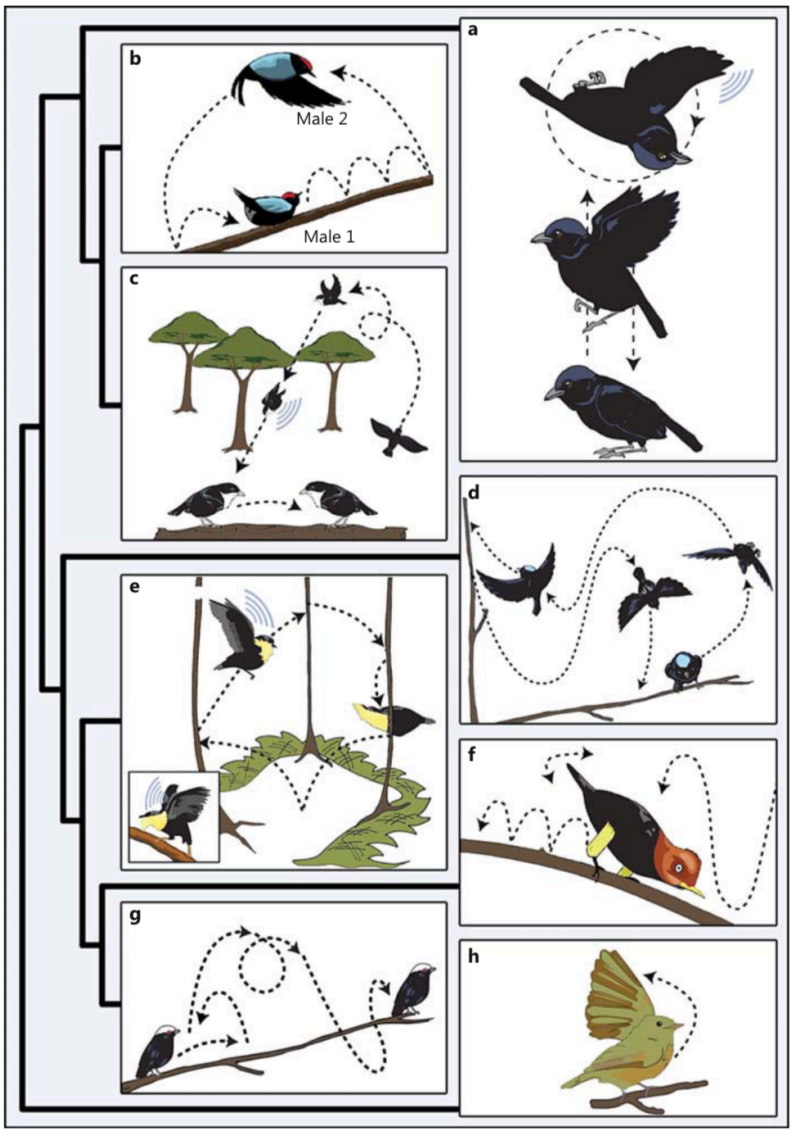

Figure 1: Figure and figure legend are modified from Lindsay, et. al 2015 and reused with permission from S. Karger AG, Basel. Manakin displays and phylogenetic relationships, with one species per genus illustrated and similarities to congeners noted. **a)** *X. atronitens:* a male performs a backflip including a wingsnap sonation. **b)** *C.*

lanceolata: two males cooperatively perform a 'cart wheel' display in which each male flutters backwards over their partner, lands and hops up to take the other's place; only one male mates. The *C. pareola* display is similar. **c)** *C. altera:* a male performs an 'above-the-canopy flight' followed by a plummeting 'log approach' with wing sonation; the male lands on the 'gardened' display log and performs a rapid 'about face'. The *C. gutturalis* display is similar, with the addition of exposed throat ruff and white wing patches. **d)** *L. coronata:* a male performs swooping 'butterfly' or 'frenzied' flights between perches, with an aerial turn to land facing the opposite direction; sometimes males 'bow' or perform an about-face pivot. The *L. suavissima* display is similar, with the addition of wing sonations and a 'slide- down' display performed on a vertical sapling. **e)** *M. vitellinus:* a male hops or flips between saplings and the ground on a cleared arena, loudly snapping his wings, lands with 'beard out', slides down a twig and produces a 'grunt' with the wings prior to copulation. **Inset** 'Rollsnap'; a series of rapid wing snaps are performed perched. The *M. candei* display is similar. **f)** *P. mentalis:* a male swoops to a perch in an 'S' flight, quivers his tail and performs a 'moonwalk' by taking tiny backward hops, sometimes pivoting to moonwalk in the opposite direction. sometimes pivoting to moonwalk in a new direction. The *P. cornuta* display is similar, with a moonwalk performed by the execution of tiny backwards steps rather than hops. **g)** *D. pipra:* a male performs rapid jumps forwards and backwards on the display perch, and rapid 'to-and-fro flights' between perches. **h)** *M. oleagineus*: a male performs a simple display with frequent single wing lifts or 'flicks', 'hops' between perches and produces undulating flights similar to manakin butterfly flights.

Purkinje Layer Measurements

Using Stereologer software (Stereologer Resource Center, Inc., St. Petersburg, Florida, USA) we obtained unbiased estimates (Mouton, 2011) of Purkinje cell layer volume, Purkinje cell number, and cell volume. Live imaging of the Nissl stained brain sections were obtained via an imi-tech IMC-3145FT camera (Carl Zeiss, Inc., Thornwood, N.Y., USA) attached to either an upright Zeiss Axio Imager M1or a Zeiss Stemi 2000-CS stereo microscope. We measured the Purkinje cell layer using the 1.25x objective on either the stereoscope or the upright microscope. We used 100x oil objective to identify cells and quantify section thickness. The final magnification factor for Stereologer calculations is determined by calibrating each objective to the dimensions of the image projected on the monitor, it is approximately 10 times the objective

magnification as the phototube magnifies 10x; 12.5x for regions and 1000x for cells and slice thickness.

We measured each CB trait in one hemi-cerebellum, starting from the most lateral section containing the cerebellum and continuing to the midsagittal section. Previously, we found no difference in the volume of left and right cerebellar volumes. In our sampling, we selected the left or right hemi-cerebellum based on which side had the best histology, while also attempting to balance left and right samples across species and individuals (Left=23, Right=15). We sampled 10-15 brain sections per individual (more samples for larger brains) at sampling intervals of 270-450 μm apart.

For all three measurements, the cerebellum was projected onto the monitor using the 1.25x objective. Stereologer then overlays a point grid on the image of the section (See Fig. 2). The initial grid shows the sample locations for cell counts and cell volume measurements as designated by your selection of distance between sampling frames (100μm). On this grid, we identified the Purkinje cell layer as the region of interest (ROI) by outlining the layer. A second grid, with the area per point from 89787.27μm - 94445.21637μm (more points for fewer sections) was used to estimate Purkinje cell layer volume using the Cavalieri point counting method (Mouton, 2011). For point counting, the number of points that fall within the PC layer are used to estimate the area of the Purkinje cell layer. To estimate volume, the thickness of each slice is also measured. Because measurements are performed after staining processes are completed, shrinkage creates variation between the thickness setting used to slice the tissue and the actual thickness of the measured slice (Mouton, 2011). Section thickness was measured using the Zeiss M1, by calculating the change in the Z-axis from the first cells to come in

focus to the last cells to come in in focus. The volume of the Purkinje cell layer (V_{ref}) in each section was calculated using the formula:

$$V_{ref} = (k \times t) \times \mathbf{\Sigma}P \times [a(p)/M^2]$$

where k= sampling interval, t= average section thickness, and **Σ**P is the sum of the points counted, a(p) is area per point (a=area, p=the number of points within that area), and M is the magnification (Mouton, 2011). M is determined by the magnification calibrations.

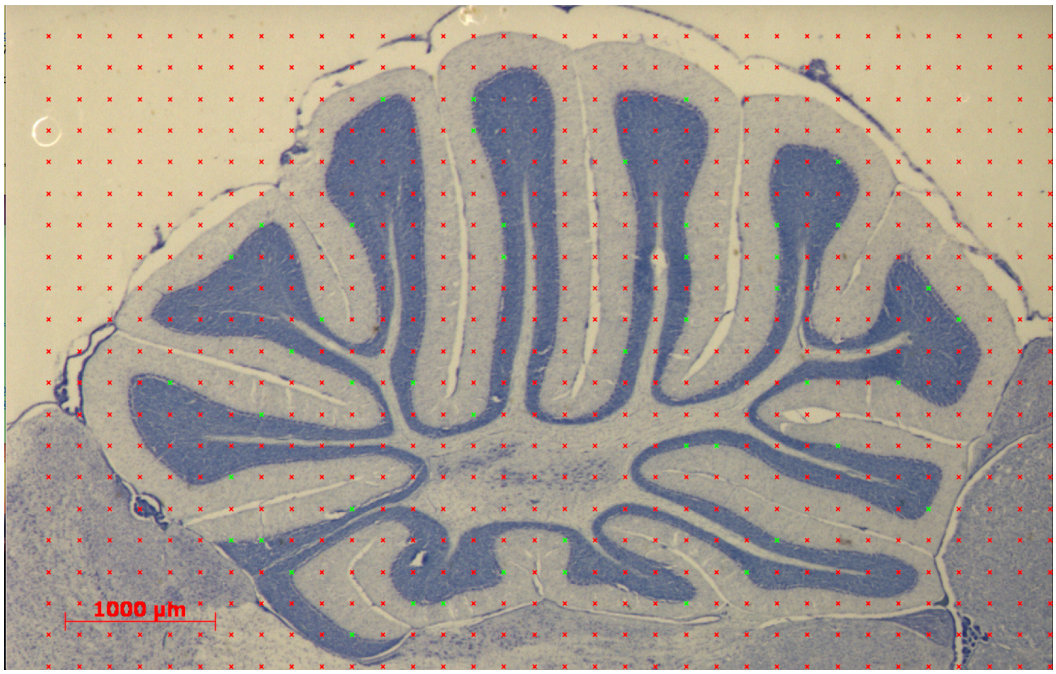

Figure 2: Low power image of cerebellum with overlying point grid for Cavalieri estimates. Grid Points that contact the Purkinje cell layer were selected to be part of the region of interest and indicated by green coloration.

We estimated total cell number using the optical fractionator. Stereologer moves the stage to each sampling location in your ROI and lays a frame with "exclusion lines" over the image (see figure 3; Mouton, 2011). All cells that appear as you focus through the Z-axis that fall do not touch the exclusion lines are counted. Section thickness is measured as for PCLvol. The total cell number is estimated (N_{obj}) with the equation:

$$N_{obj}=\Sigma Q \times 1/SSF \times 1/ ASF \times 1/ TSF$$

where **Σ**Q is the sum of cells counted, SSF is the section sampling fraction (number of sections sampled/total number of sections in region of interest), ASF is the area sampling fraction (area of the counting frame/ area of monitor viewing window), and TSH is the thickness sampling fraction (height of the sample/ total section thickness) (Mouton, 2011). When setting the thickness of your section, a guard area at the top at the bottom of the section is not measured to ensure only whole cells are counted, the section thickness minus this guard area is your sample height. The total area sampled and the total number of sections in the reference space is dependent on the amount of grid points selected to be within the region of interest at 1.25x magnification.

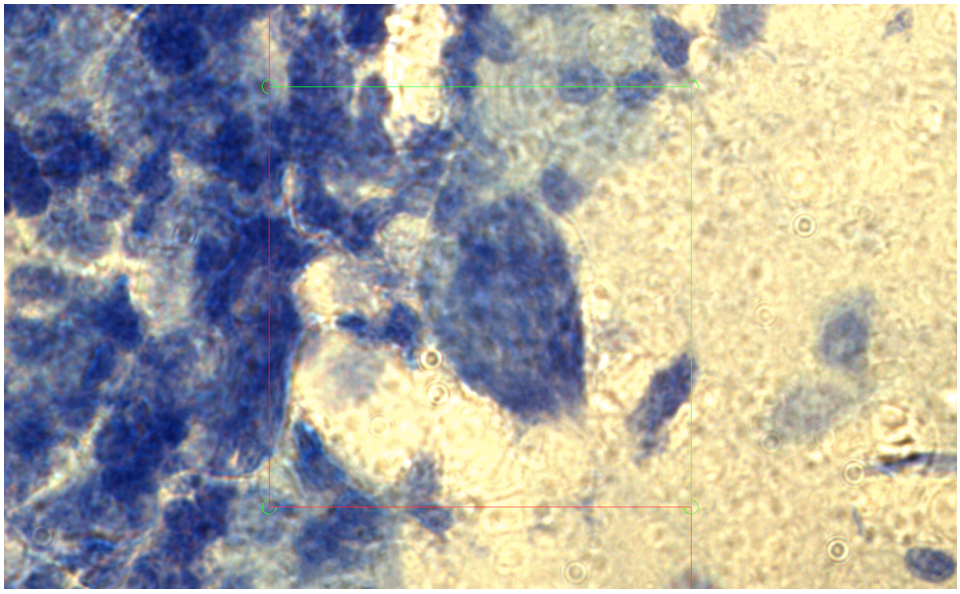

Figure 3: Example of frame with Lines of Inclusion and Exclusion at 100x oil immersion magnification. Any cells outside of or touching red (left) lines were excluded from counts and measurements, while cells within the box or making contact with the green lines (right) were included in counts and measurements.

We quantified Purkinje cell volume using isotropic rotator method for thin tissue sections (30µm and less). The Isotropic Rotator method estimates cell volume by placing

line at a random angle on a cell, the user then defines the length of the cell by marking the top and bottom of the cell intersecting these points. Three lines perpendicular to the first then appear and the points of intersection along the lines are marked to estimate cell perimeter. Cell volume is calculated using the formula:

$$V_{obj} = (4\Pi \text{ x mean } l^3/3)$$

Where l = the length of the cell and the number of grid lines used for measurement.

Sampling Parameters

To obtain coefficient of error (CE) values of 0.052 (PCLvol), 0.219 (PCnum), and 0.037 (PCvol), we sampled 10-15 brain sections per individual (more samples for larger brains) at sampling intervals of 270-450μm apart with area per point calibrated for the 1.25x objective for each scope varying from 89787.27μm - 94445.21637μm (more points for fewer sections) and counted 1145 number cells with counting frames for cell counts and cell volumes spaced at 1000μm. (Marcos, 2012). The coefficient of error is a statistical value that accounts for biological variability and variance between measurements, providing a quantitative likelihood that a measurement can be repeated (Mouton, 2011).

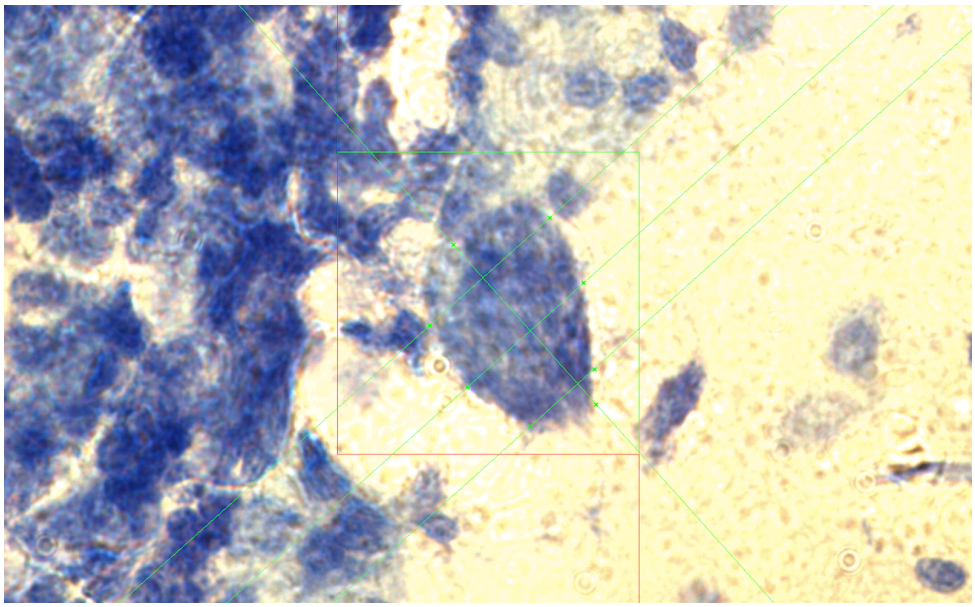

Figure 4: Isotropic Rotator probe used to measure volume of Purkinje cells. Red and green lines represent lines of inclusion and exclusion. Probe lines are placed at random angles and used to measure the length and size of cell by marking the points on the probe line that fall on the perimeter of the cell.

Statistical Analysis

Allometric Scaling

Because brain regions are assumed to grow in scale with one another, and because larger animals are known to have larger brains, standard practice would call for using marginal means (Day et. al, 2016) or residual analysis (Gutierrez-Ibanez, et al., 2016) to statistically adjust the size of the Purkinje cell layer volume for body mass or for the size of the region in which it is contained, either cerebellar volume minus Purkinje cell layer volume (CBvol-PCLvol) or whole brain volume minus Purkinje cell layer volume (WBvol-PCLvol). However, exactly which statistical method should be used for these adjustments has long been debated (Darlington, et al., 2001) and recently, several authors have called the entire practice of adjustment into question (Day, et al., 2016). In addition, our data set offers special challenges as each of the mathematical models assume

independent variation between display complexity and features used to adjust for variation in animal size, CB-PCLvol, and body mass. In our data set, we already know that several neuroanatomical features, and quite uniquely in the literature, body mass are positively associated with display complexity (Lindsay, et al. 2015; Pano, 2015; Day et al., 2016, Helmhout, 2016). To preempt concerns of the ongoing scaling debate, we examined PCLvol using both residual analysis and marginal means analysis. We examined correlations of log-transformed body mass (g), log-transformed volumes of neuroanatomical features (μ^3, measured in previous studies) (Day, et al. 2016; Helmhout, 2016; Pano, 2015) and display complexity to determine if any variables not associated with display complexity were correlated with PCLvol and could be used to adjust for allometry (see table 3). Only nucleus taeniae (NTn) was marginally correlated with PCLvol ($R=0.525$, $p=0.065$) but not correlated with display complexity ($R=0.22$, $p=0.469$). We calculated the marginal means of brain size from a general linear model (GLM) with log-transformed PCLvol (μ^3) as the dependent variable, species as a fixed factor ($n=13$), and log-transformed NTn-PCLvol(μ^3) as a covariate. In GLM, the covariate must not be correlated with the independent variable (species), thus; the GLM is run first with the interaction term, this being non-significant ($F(12,38)=0.491$,$p=0.884$), the GLM is run again without the interaction term. The resulting marginal means were used in subsequent analysis as our measure of PCL-size-adjusted relative PCLvol. Similarly, we also obtained mean residuals from a least squares regression analysis, PCLvol regressed on nucleus taeniae volume minus Purkinje cell layer volume (NTn-PCLvol), to obtain residual PCLvol. For completeness, we ran these same analyses using

body mass (g) and CB-PCLvol (μ^3) as covariates and found results and interpretations unchanged (data not shown).

Interrelationships Among Brain Regions

To examine relationships among CB variables and other brain regions, we examined the pairwise correlations between CBvol-PCLvol, PCLvol, PCnum, and PCvol and body mass (g) other brain regions measured previously (Lindsay, et al. 2015; Pano, 2015, see table 3). All region volumes and body weight were log transformed.

Relationship of PC variables to Display Complexity

We ran independent regressions of adjusted and residual PCLvol on display complexity (see table 4). In addition, the solution to the scaling debate seems to use both raw volumes as well as adjusted and residual values to help interpret the full biological significance of relationships and to examine cell counts rather than volumes to understand how brain regions' processing power relates to behaviors. Thus, we also regressed PCLvol, PCnum and PCvol on display complexity being mindful of our smaller sample size for estimates of cell number and cell volumes (see table 4).

Phylogenetic Correction

Because species can not be considered independent variables, one must adjust for the phylogenetic relationships among species. While we have not yet performed a phylogenetically corrected analysis for our PC variables, previous examination of phylogenetically corrected and uncorrected relationships has not altered the statistical significance nor the interpretation of relationships (see table 5). Thus, we expect to find

similar results for PC variables in relation to other morphological measurements and related to complexity. This is, with the exception of PCnum as the species that falls furthest from the regression line is the ochre-bellied flycatcher (see figure 6), the least related to the other species.

Relationship of all brain region variables to Display complexity

Our full data set (see table 3) includes a number of variables that are highly intercorrelated. While this is somewhat to be expected with brain regions if allometric scaling rather than mosaic evolution is the principal force shaping growth, it is very unusual to see brain region variables that are related to behavior. These interrelationships also make it difficult to create models of the best predictors of complexity. In addition, it is necessary for models to be adjusted for phylogenetic relationships, which adds computational difficulties for modeling to concerns related to meeting the mathematical assumptions of models. However, given that phylogenetic signal has been relatively weak in previous models and with some cautions as to our methods for making variables more independent of one another, we ran a series of stepwise regressions to determine which variables would enter into a model of predicting display complexity. We subtracted for each brain region volume the volume of other brain regions contained with in the region. For example, since arcopallium, and cerebellum were in the model, we would subtract from whole brain volume the volume of both of these regions. Given all the difficulties already expressed with traditional methods for adjusting for body size, we did not attempt to enter adjusted values in our regressions. While we do not consider these analyses to be definitive, they offer preliminary models of variables that best predict display complexity. We ran three stepwise regressions. The first included all variables that are

related to complexity (see table 6). In the second, we removed one body size measure, tarsus cubed. In the third, we removed body mass, so that the model no longer included a measurement of body size. In the last regression, we examined only measurements of brain regions. See table 6 for stepwise regression results.

Results

PC variables showed no intercorrelation among any measured brain variables. Purkinje cell layer volume had no significant relationship with display complexity, but when Purkinje cell layer volume was removed from cerebellar volume (CBvol-PCLvol), a positive relationship with PCLvol was observed (see Table 3 for statistical results). Correlation analysis showed that Purkinje cell number was positively related to display complexity upon exclusion of the MIOL outgroup. We present results of correlation analyses in table 3 and figures 5-7 and results of the regression analyses in tables 4-6. Regression analysis against display complexity of variables that have been phylogenetically corrected is presented in table 5.

Table 3: Correlations between PC variables, Display Complexity, and Brain Regions

		PCLVol	PCnum	Pcvol	CbminPCL	TN	BrminCB	LnAP	NucRot	Wtg	Tar3
Comp	R	0.32	0.694	-0.363	0.547	0.22	0.447	0.541	0.477	0.567*	0.650*
	p	0.286	0.084	0.423	0.053	0.469	0.125	0.056	0.099	0.043	0.022
PCLVol	R		0.434	-0.015	0.718**	0.525	0.506	0.575*	0.331	.0.590*	0.49
	p		0.331	0.974	0.006	0.065	0.078	0.04	0.27	0.034	0.106
PCnum	R			-0.531	0.234	-0.616	0.123	0.469	0.279	0.398	-0.019
	p			0.22	0.614	0.141	0.793	0.288	0.544	0.377	0.971
Pcvol	R				0.386	0.741	0.572	0.315	-0.216	0.304	0.379
	p				0.392	0.057	0.18	0.491	0.641	0.508	0.458
CbminPCL	R					0.797**	0.869**	0.913**	0.744**	0.828**	0.786**
	p					0.001	0.000114	0.000013	0.004	0.000467	0.002
TN	R						0.806**	0.724**	0.644*	0.787**	0.585*
	p						0.001	0.005	0.018	0.001	0.046
HemiBrminCB	R							0.882**	0.616*	0.864**	0.698*
	p							0.000068	0.025	0.000142	0.012
AP	R								0.742**	0.852**	0.816**
	p								0.004	0.000221	0.001
NucRot	R									0.723**	0.745**
	p									0.005	0.005
Wtg	R										0.766**
	p										0.004
Tar3	R										
	p										

*Correlation is significant at .05 level
**Correlation is significant at .01 level
R values represent the strength of correlation between variables, ranging from -1 to 1. P values represent significance of relationship, with $p<0.05$ representing a significant relationship. Highlighted cells with black borders are relationships between PC variables and display complexity, highlighted cells with red borders are relationships between covariate nucleus taeniae and display complexity and Purkinje cell layer volume.

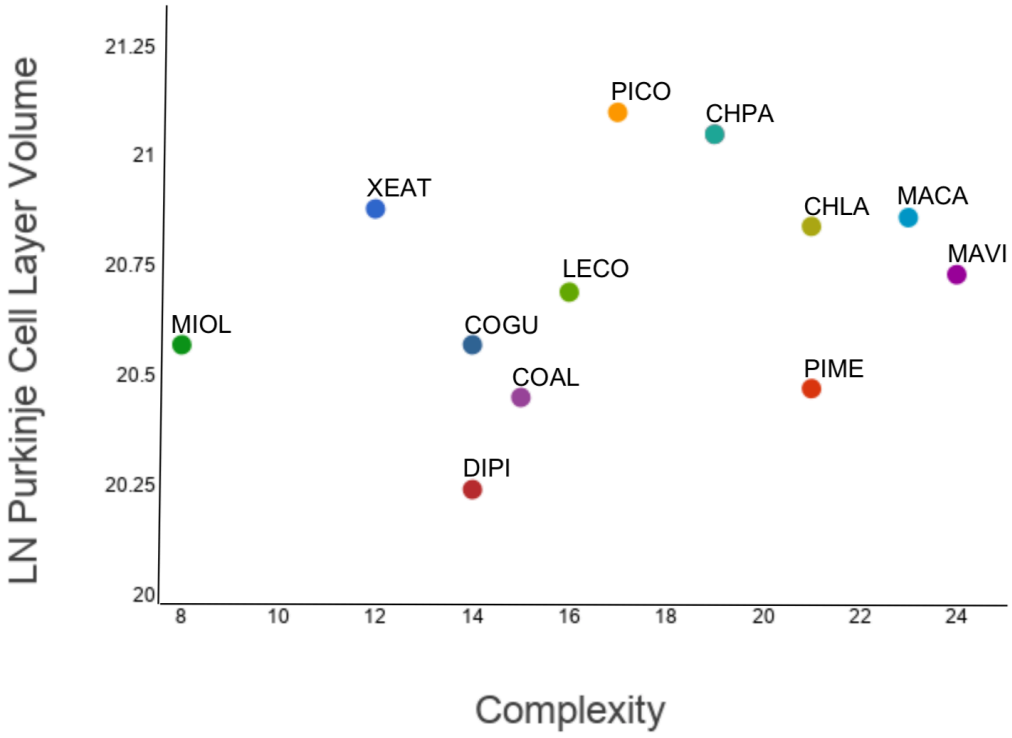

Figure 5: Correlation Analysis of Purkinje Cell Layer Volume vs. Display Complexity

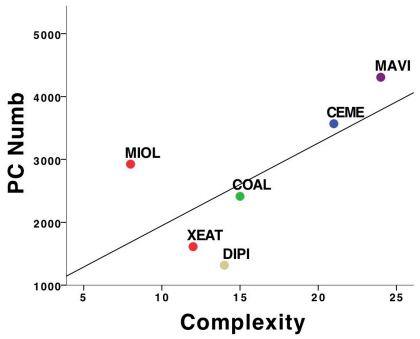

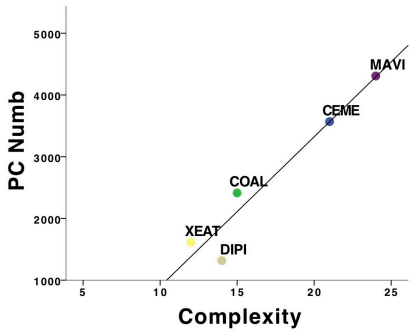

Figure 6: Correlation of Purkinje cell number vs. display complexity including MIOL outgroup. Figure 7: Correlation of Purkinje cell number vs. display complexity excluding MIOL outgroup.

Table 4: Regression of Purkinje Cell Variables with Display Complexity

Independent Variable	R^2	t	p
Purkinje Cell Layer Volume Residuals	0.276	2.046	0.065
Purkinje Cell Volume	0.132	3.054	0.028
Purkinje Cell Number (with MIOL)	0.481	1.379	0.084
Purkinje Cell Number (without MIOL)	0.871	3.813	0.007

We first found correlations between PCvol, PCLvol, PCnum, and display complexity. In the correlation between PCnum and display complexity, the MIOL outgroup fell off the line of best fit between PCnum and complexity. Because the MIOL outgroup was an outlier from the regression line, a regression was run excluding MIOL. Upon running a regression without MIOL, a large difference in the significance of the relationship between PCnum and display complexity was found (R^2=0.871, p=0.007) despite the fact that removing a sample reduced our power. With the regression, we ran casewise diagnostics to find that MIOL is over one standard deviation outside of the residuals for other species. Relationships between complexity and other CB variables and

between CB measurements and other brain and body measurements changed very little when we excluded the MIOL outgroup, with none that were previously significant becoming insignificant, with the exception of one that was marginally significant (probably due to the loss of power).

Table 5: Phylogenetically corrected regression of brain components and display complexity

Independent Variable	Allometric Factor	R^2	t	p	MLλ
Brain Vol Marginal Means	Body Weight	0.23	2.15	0.05	0
Brain Vol Residuals	Body Weight	-0.08	0.25	0.81	0
Brain Wt Marginal Means	Body Weight	0.37	2.84	0.02	0
Brain Wt Residuals	Body Weight	-0.08	0.36	0.72	0
Cerebellum Marginal Means	Brain-Cerebellum	0.23	2.16	0.05	0
Cerebellum Residuals	Brain-Cerebellum	0.22	2.08	0.06	0
Arcopallium Marginal Means	Brain-AP Tn	0.25	2.24	0.05	0
Arcopallium Residuals	Brain-AP Tn	0.18	1.91	0.08	0
Nucleus Taenia Marginal Means	Brain-Tn Vol	-0.02	0.89	0.39	0*
Nucleus Taenia Residuals	Brain-Tn Vol	0.09	-0.06	0.96	0
Nucleus Rotundus Marginal Means	Brain-Cb-Ap-Tn-NR	0.01	0.38	0.73	
Nucleus Rotundus Residuals	Brain-Cb-Ap-Tn-NR	-0.08	0.35	0.71	
Body Weight		0.26	2.29	0.04	0*
Brain Weight		0.37	2.84	0.02	0
Brain Volume		0.22	1.78	0.10	
Tarsus cubed		0.49	5.88	0.00	

After variables were phylogenetically corrected, there was not a difference in which relationships were significant and which were not, suggesting that after phylogenetic correction, Purkinje cell relationships will remain the same. This is with the exception of the PCnum. Once phylogenetically corrected, the relationship between PCnum and display complexity may change from marginally significant ($p=0.08$) to significant ($p<0.05$).

Table 6: Stepwise Regression of Variables Positively Related to Display Complexity

Variable	R^2	p
Tarsus	0.423	0.022
Body Weight	0.322	0.043
Arcopallium (minus Nucleus taeniae)	0.250	0.047

Initially, all variables with a positive relationship with display complexity were included in stepwise regression, resulting in tarsus as the strongest predictor of display complexity. For modeling the second stepwise regression, tarsus was excluded, and body weight was observed to be the second strongest predictor. For the third regression, both tarsus and body weight were excluded, and arcopallium value was observed as the next strongest predictor of display complexity.

Figures 5-7: Correlation Analyses of Purkinje Cell layer volume, Purkinje cell number with MIOL outgroup, and Purkinje cell number excluding MIOL outgroup vs. display complexity. Species data points are labeled with 4-letter abbreviations of species name (LECO=*L. coronata*, CHPA=*C. pareola*, COGU=*C. gutteralis*, DIPI=*D. pipra*, MAVI=*M. vitellinus*, LESU=*L. suavissima*, CHLA=*C. lanceolata*, CECO=*C. cornuta*, CEME=*C. mentalis*, MACA=*M.candei*, COAL=*C. altera*, XEAT=*X. atronitens*, MIOL=*M. oleagineus*)

Discussion

Among the 13 species examined for Purkinje cell layer and 6 species examined for Purkinje cell volume, we found that there was no relationship between Purkinje cell volume or Purkinje cell layer volume and display complexity. In a focal subset of 6 species, we found that, once the outgroup was removed, the Purkinje cell number, but not Purkinje cell volume, increased with increasing display complexity. These results support previous studies that found positive relationships between display complexity and brain weight, body weight, tarsus size, arcopallium volume, and cerebellar volume (Lindsay, et al., 2015; Pano, 2015; Helmhout, 2016). Because the cerebellum plays a prominent role in coordinated movement and has a known positive relationship with display complexity, we tested for a positive relationship between one of the measured Purkinje cell layer variables and display complexity. While our study was limited to the Purkinje cell layer, and the cerebellar cortex also consists of the molecular and granular layer, we are able to discuss the possible implications of the role the remaining layers of the cerebellum play as a whole by subtracting the Purkinje cell layer volume from total cerebellar volume.

The Purkinje cell layer volume showed no relationship with display complexity, PCvol, or PCnum. Because there was no relationship between PCLvol and PCvol or PCnum, this leads us to believe that the Purkinje cell layer volume possibly expands by increasing space between Purkinje cells or increasing glia within the layer. Once the PCLvol was removed from the total cerebellar volume, a positive relationship was found between CBvol-PCLvol and PCLvol. The remaining layers in the cerebellar cortex, the molecular and granular layer, both play important roles in signal processing. Granular cells receive most of the input of the cerebellum (Sultan, et al., 2007). They act with the

Golgi, stellate, and basket cells to provide inhibitory regulation of Purkinje cells (Albus, 1971; Voogd, et al., 1998). This finding implies that, while cerebellar cortex output is important, the cerebellar processing of signals may play a more important role in manakin display production.

Purkinje cells are the sole output of the cerebellar cortex, and receive excitatory input from two sources: parallel fibers and climbing fibers (Konnerth, et al., 1990; Devi, et al., 1016). While Purkinje cells can receive input from upwards of 80,000 parallel fibers (Konnerth, et al. 1990), they have a known small ratio with climbing fibers in which only one or two synapse with each Purkinje cell (Devi, et al., 2016). This relationship raises the possibility that the positive relationship between Purkinje cell number and display complexity may serve to accommodate for increased excitatory signals from climbing fibers while maintaining the small synapsing ratio.

In determining measurement methods for Purkinje cell morphology, we decided to perform measurements uniformly across the entire cerebellum instead of measuring Purkinje cells per folia. While it was previously thought that each folia played a distinct role in display production, it was found that the neuroanatomical relationship of specific folia to behaviors is unlikely to be consistent across species when the number of folia varies within species (Wilkening, 2011). This leads us to believe that individual folia either have little importance in display production, or that certain folia may have a distinguished relationship between number of Purkinje cells and either brain weight or display complexity.

Cerebellar regions, however, have a known role in manakin display production and pose an interesting area for future studies. The cerebellum is divided into three

regions: anterior, posterior, and vestibular. Each region plays a distinct role in manakin display production: the anterior cerebellum controls the hindlimbs, the posterior cerebellum controls flights, and the vestibular region impacts balance (Iwaniuk 2006b, 2007; Whitlock, 1952). Studies of Purkinje cell density in these different regions may lead to interesting findings on the importance of cerebellar output in each region.

As previously stated, we have found that cerebellar volume increases in tandem with display complexity (Pano, 2015). Our results show that this relationship is preserved in CBvol-PCLvol, whereas Purkinje cell layer volume does not preserve this relationship. These results suggest that either Purkinje cell layer volume is less relevant to manakin display production than the rest of the cerebellum, or that cerebellar regions work so in concert in display production that the relationship to complexity cannot be detected in individual layer measurements. The positive relationship between CBvol-PCLvol and display complexity also raises the possibility that there is a lack of allometric scaling among layers within the cerebellum. This possibility leads us to ask: are we observing is a lack of relationship between Purkinje cell layer volume and complexity, or are we only seeing a positive relationship with CBvol-PCLvol because it is so closely related with variables that are already known to have a positive relationship with display?

Future studies of Purkinje cell morphology and display complexity will aim to further quantify the relationships between cerebellar components and display complexity by counting and measuring the cells of the granular and molecular layer in the cerebellar cortex, as well as counting and measuring the deep cerebellar nuclei. Because a known numerical relationship has been established between Purkinje cells and the deep cerebellar nuclei on which they project, we expect that with our finding of a positive

relationship with Purkinje cell number and display complexity, there will also be a positive relationship between deep cerebellar nuclei number and display complexity. It has been previously found that the different types of deep cerebellar nuclei: dentate, interposed, and fastigial, show different efferent projection patterns (Asanuma, 1982). It is of interest to determine which type of deep cerebellar nuclei have a relationship with Purkinje cell number and also with display complexity. Obtaining this information will allow us to further understand what neural and motor pathways are strongly influencing mating display complexity in Manakins.

Future analyses will be performed to determine which variable is the most important in manakin display production. We have a large data set with many measurements of brain regions- five of which have shown to have positive relationships with display complexity. Of the variables with a positive relationship with display complexity, brain weight, body weight, tarsus size, arcopallium volume, cerebellar volume, and Purkinje cell number, we hope to find out which is most important by using a multivariate model to analyze relationships (Lindsay et al., 2015; Pano, 2015; Day, et al. 2016; Helmhout, 2016).

While this study lacks complete measurement of cell count and cell volume in many subjects, and lacks analyses that require a larger sampling number, its results are still important. The finding that Purkinje cell number has a positive relationship with display complexity shows us that cerebellar output is important in manakin display production, and that the number of cells rather than a volume measurement of the whole layer or the volume of the cells is what drives the positive relationship between cerebellar volume and display complexity.

Bibliography

Acerbo, M. J., Lazareva, O. F., McInnerney, J., Leiker, E., Wasserman, E. A., & Poremba, A. (2012). Figure-ground discrimination in the avian brain: The nucleus rotundus and its inhibitory complex. *Vision Research, 70*, 18-26. doi:10.1016/j.visres.2012.07.023

Albus, J. S. (1971). A theory of cerebellar function. *Mathematical Biosciences, 10*(1-2), 25-61. doi:10.1016/0025-5564(71)90051-4

Barske, J., Schlinger, B. A., Wikelski, M., & Fusani, L. (2011). Female choice for male motor skills. *Proceedings of the Royal Society B: Biological Sciences, 278*(1724), 3523-3528. doi:10.1098/rspb.2011.0382

Borgia, G., Borgia, G., Mueller, U., & Mueller, U. (1992). Bower destruction, decoration stealing and female choice in the spotted bowerbird chlamydera maculata. *Emu, 92*(1), 11-18. 10.1071/MU9920011

Bostwick, K. S. (2003). High-speed video analysis of wing-snapping in two manakin clades (Pipridae: Aves). *Journal of Experimental Biology, 206*(20), 3693-3706. doi:10.1242/jeb.00598

Butler, A. B., & Hodos, W. (1996). Comparative vertebrate neuroanatomy: Evolution and adaptation. 10.1002/0471733849

Camilli, P. D., Miller, P., Levitt, P., Walter, U., & Greengard, P. (1984). Anatomy of cerebellar Purkinje cells in the rat determined by a specific immunohistochemical marker. *Neuroscience, 11*(4). doi:10.1016/0306-4522(84)90193-3

Chapman, Frank M. (Frank Michler), & Chapman Expedition to the Canal Zone (1931-1935). (1935). The courtship of gould's manakin (manacus vitellinus vitellinus) on barro colorado island, canal zone. *Bulletin of the American Museum of Natural History,* , 471.

Clayton, N. S. (1998). Memory and the hippocampus in food-storing birds: A comparative approach. *Neuropharmacology, 37*(4), 441-452. 10.1016/S0028-3908(98)00037-9

Darlington, R. B., & Smulders, T. V. (2001). Problems with residual analysis. *Animal Behaviour, 62*(3), 599-602. 10.1006/anbe.2001.1806

Day, L. B., Westcott, D. A., & Olster, D. H. (2005). Evolution of Bower Complexity and Cerebellum Size in Bowerbirds. *Brain, Behavior and Evolution, 66*(1), 62-72. doi:10.1159/000085048

Day, L. B., Fusani, L., Hernandez, E., Billo, T. J., Sheldon, K. S., Wise, P. M., & Schlinger, B. A. (2007). Testosterone and its effects on courtship in golden-collared manakins (manacus vitellinus): Seasonal, sex, and age differences. Hormones and Behavior, 51(1), 69-76. 10.1016/j.yhbeh.2006.08.006

Day, L. B., Fusani, L., Kim, C., & Schlinger, B. A. (2011). Sexually dimorphic neural phenotypes in golden-collared manakins (manacus vitellinus). *Brain, Behavior and Evolution, 77*(3), 206-218. 10.1159/000327046

Day, L. B., & Lindsay, W. R. (2016). Associations between manakin display complexity and both body and brain size challenge assumptions of allometric correction: A response to gutierrez-ibanez et al. (2016). *Brain, Behavior and Evolution, 87*(4), 227-231. 10.1159/000446341

Devi, S. P. S., Howe, J. R., & Auger, C. (2016). Train stimulation of parallel fibre to purkinje cell inputs reveals two populations of synaptic responses with different receptor

signatures: Two populations of parallel fibre inputs to purkinje cells. *The Journal of Physiology, 594*(13), 3705-3727. 10.1113/JP272415

Durães, R., Loiselle, B. A., & Blake, J. G. (2007). Intersexual spatial relationships in a lekking species: Blue-crowned manakins and female hot spots. *Behavioral Ecology, 18*(6), 1029-1039. 10.1093/beheco/arm072

Duval, E. H. (2007). Cooperative Display And Lekking Behavior Of The Lance-Tailed Manakin (Chiroxiphia Lanceolata). *The Auk, 124*(4), 1168. doi:10.1642/0004-8038(2007)124[1168:cdalbo]2.0.co;2

Fusani, L., Day, L. B., Canoine, V., Reinemann, D., Hernandez, E., & Schlinger, B. A. (2007). Androgen and the elaborate courtship behavior of a tropical lekking bird. *Hormones and Behavior, 51*(1), 62-68. doi:10.1016/j.yhbeh.2006.08.005

Fusani, L., Donaldson, Z., London, S. E., Fuxjager, M. J., & Schlinger, B. A. (2014). Expression of androgen receptor in the brain of a sub-oscine bird with an elaborate courtship display. *Neuroscience Letters, 578*, 61-65. doi:10.1016/j.neulet.2014.06.028

Goldowitz, D. (1998). The cells and molecules that make a cerebellum. *Trends in Neurosciences, 21*(9), 375-382. doi:10.1016/s0166-2236(98)01313-7

Gutierrez-Ibanez, C., Iwaniuk, A. N., & Wylie, D. R. (2016). Relative brain size is not correlated with display complexity in manakins: A reanalysis of lindsay et al. (2015). *Brain, Behavior and Evolution, 87*(4), 223-226. 10.1159/000446312

Hall, Z. J., Street, S. E., & Healy, S. D. (2013). The evolution of cerebellum structure correlates with nest complexity. *Biology Letters, 9*(6), 20130687-20130687. 10.1098/rsbl.2013.0687

Helmhout, Wilson (2016) *Females Influence Brain Evolution: Dance Complexity Related to Volume of a Sensorimotor Region in Manakins.*

Iwaniuk, A. N., Hurd, P. L., & Wylie, D. R. W. (2006). Comparative morphology of the avian cerebellum: I. degree of foliation. *Brain, Behavior and Evolution, 68*(1), 45-62. 10.1159/000093530

Konnerth, A., Llano, I., & Armstrong, C. M. (1990). Synaptic currents in cerebellar purkinje cells.*Proceedings of the National Academy of Sciences of the United States of America, 87*(7), 2662-2665. 10.1073/pnas.87.7.2662

Lindsay, W. R., Houck, J. T., Giuliano, C. E., & Day, L. B. (2015). Acrobatic Courtship Display Coevolves with Brain Size in Manakins (Pipridae). *Brain, Behavior and Evolution, 85*(1), 29-36. doi:10.1159/000369244

Madden, J. R. (2003). Bower decorations are good predictors of mating success in the spotted bowerbird. *Behavioral Ecology and Sociobiology, 53*(5), 269-277. 10.1007/s00265-003-0583-6

Marini, M. A. (1992). Foraging Behavior and Diet of the Helmeted Manakin. *The Condor, 94*(1), 151-158. doi:10.2307/1368804

Marshall, AJ (1954) Bower-Birds: Their Displays and Breeding Cycles. Oxford UK: Clarendon Press.

Marshall, R. C., Buchanan, K. L., & Catchpole, C. K. (2003). Sexual selection and individual genetic diversity in a songbird. *Proceedings of the Royal Society B: Biological Sciences, 270*(Suppl_2). doi:10.1098/rsbl.2003.0081

Mouton, Peter R (2011). The Stereologer Handbook: Introduction to Unbiased Stereology and Stereologer User's Guide.

Nottebohm, F., & Arnold, A. (1976). Sexual dimorphism in vocal control areas of the songbird brain. *Science, 194*(4261), 211-213. doi:10.1126/science.959852

Palkovits, M., Magyar, P., & Szenta´gothai, J. (1972). Quantitative histological analysis of the cerebellar cortex in the cat. IV. Mossy fiber-purkinje cell numerical transfer. *Brain Research, 45*(1), 15-29. doi:10.1016/0006-8993(72)90213-2

Pano, G., Lindsay W.R., Day, L.B. (2015): Do the Sexiest Dancers Have the Largest Little Brain?: Associations between display complexity and both brain volume and cerebellar granular layer volume in manakins (Pipridae). Abstract, *Society of Neuroscience.*

Prum, R. O. (1990). Phylogenetic Analysis of the Evolution of Display Behavior in the Neotropical Manakins (Aves: Pipridae). *Ethology, 84*(3), 202-231. doi:10.1111/j.1439-0310.1990.tb00798.x

Prum, R. O. (1994). Phylogenetic Analysis of the Evolution of Alternative Social Behavior in the Manakins (Aves: Pipridae). *Evolution, 48*(5), 1657. doi:10.2307/2410255

Prum, R. O. (1998). Sexual selection and the evolution of mechanical sound production in manakins (Aves: Pipridae). *Animal Behaviour, 55*(4), 977-994. doi:10.1006/anbe.1997.0647

Reiner, A., Perkel, P. J., Mello, C. V., Jarvis, E. D. (2004): Songbirds and the revised avian brain nomenclature. Ann. New York Academy of Science 1016: 77-108

Schlinger, B. A., Barske, J., Day, L., Fusani, L., & Fuxjager, M. J. (2013). Hormones and the neuromuscular control of courtship in the golden-collared manakin (Manacus vitellinus). *Frontiers in Neuroendocrinology, 34*(3), 143-156. doi:10.1016/j.yfrne.2013.04.001

Sherry, D. F. (2011). The hippocampus of food-storing birds. *Brain, Behavior and Evolution, 78*(2), 133-135. 10.1159/000330314

Snow, B. K., & Snow, D. W. (1979). The Ochre-Bellied Flycatcher and the Evolution of Lek Behavior. *The Condor, 81*(3), 286. doi:10.2307/1367635

Sugihara, I. (2010). Compartmentalization of the Deep Cerebellar Nuclei Based on Afferent Projections and Aldolase C Expression. *The Cerebellum, 10*(3), 449-463. doi:10.1007/s12311-010-0226-1

Sultan, F., & Glickstein, M. (2007). The cerebellum: Comparative and animal studies. *The Cerebellum, 6*(3), 168-176. 10.1080/14734220701332486

Thach, W. T., Goodkin, H. P., & Keating, J. G. (1992). The cerebellum and the adaptive coordination of movement. Annual Review of Neuroscience, 15, 403-442.

Voogd, J., & Glickstein, M. (1998). The anatomy of the cerebellum. *Trends in Neurosciences, 21*(9), 370-375. 10.1016/S0166-2236(98)01318-6

Westcott, D. A., & James N. M. Smith. (1994). Behavior and social organization during the breeding season in mionectes oleagineus, a lekking flycatcher. *The Condor, 96*(3), 672-683.

Whitlock, D. G. (1952). A neurohistological and neurophysiological study of afferent fiber tracts and receptive areas of the avian cerebellum. *Journal of Comparative Neurology, 97*(3), 567-635. 10.1002/cne.900970307

Wilkening, S. R., & University of Mississippi. Department of Biology. (2011). *Avian cerebellum specialization in relation to acrobatic courtship displays in manakins (pipridae)*

Yamamoto, K., et al, (2005): Subpallial amygdala and nucleus taeniae in birds resemble extended amygdala and medial amygdala in mammals in their expression of markers of regional identity. *Brain research bulletin* 66: 341-347